doi:10.1038/nature08723

LETTERS

Foot strike patterns and collision forces in habitually barefoot versus shod runners

Daniel E. Lieberman[1], Madhusudhan Venkadesan[1,2]*, William A. Werbel[3]*, Adam I. Daoud[1]*, Susan D'Andrea[4], Irene S. Davis[5], Robert Ojiambo Mang'Eni[6,7] & Yannis Pitsiladis[6,7]

Humans have engaged in endurance running for millions of years[1], but the modern running shoe was not invented until the 1970s. For most of human evolutionary history, runners were either barefoot or wore minimal footwear such as sandals or moccasins with smaller heels and little cushioning relative to modern running shoes. We wondered how runners coped with the impact caused by the foot colliding with the ground before the invention of the modern shoe. Here we show that habitually barefoot endurance runners often land on the fore-foot (fore-foot strike) before bringing down the heel, but they sometimes land with a flat foot (mid-foot strike) or, less often, on the heel (rear-foot strike). In contrast, habitually shod runners mostly rear-foot strike, facilitated by the elevated and cushioned heel of the modern running shoe. Kinematic and kinetic analyses show that even on hard surfaces, barefoot runners who fore-foot strike generate smaller collision forces than shod rear-foot strikers. This difference results primarily from a more plantarflexed foot at landing and more ankle compliance during impact, decreasing the effective mass of the body that collides with the ground. Fore-foot- and mid-foot-strike gaits were probably more common when humans ran barefoot or in minimal shoes, and may protect the feet and lower limbs from some of the impact-related injuries now experienced by a high percentage of runners.

Running can be most injurious at the moment the foot collides with the ground. This collision can occur in three ways: a rear-foot strike (RFS), in which the heel lands first; a mid-foot strike (MFS), in which the heel and ball of the foot land simultaneously; and a fore-foot strike (FFS), in which the ball of the foot lands before the heel comes down. Sprinters often FFS, but 75–80% of contemporary shod endurance runners RFS[2,3]. RFS runners must repeatedly cope with the impact transient of the vertical ground reaction force, an abrupt collision force of approximately 1.5–3 times body weight, within the first 50 ms of stance (Fig. 1a). The time integral of this force, the impulse, is equal to the change in the body's momentum during this period as parts of the body's mass decelerate suddenly while others decelerate gradually[4]. This pattern of deceleration is equivalent to some proportion of the body's mass (M_{eff}, the effective mass) stopping abruptly along with the point of impact on the foot[5]. The relation between the impulse, the body's momentum and M_{eff} is expressed as

$$\int_{0^-}^{T} F_z(t) = M_{\mathrm{body}}(\Delta v_{\mathrm{com}} + gT) = M_{\mathrm{eff}}(-v_{\mathrm{foot}} + gT) \qquad (1)$$

where $F_z(t)$ is the time-varying vertical ground reaction force, 0^- is the instant of time before impact, T is the duration of the impact transient, M_{body} is the body mass, v_{com} is the vertical speed of the centre of mass, v_{foot} is the vertical speed of the foot just before impact and g is the acceleration due to gravity at the Earth's surface.

Impact transients associated with RFS running are sudden forces with high rates and magnitudes of loading that travel rapidly up the body and thus may contribute to the high incidence of running-related injuries, especially tibial stress fractures and plantar fasciitis[6–8]. Modern running shoes are designed to make RFS running comfortable and less injurious by using elastic materials in a large heel to absorb some of the transient force and spread the impulse over more time[9] (Fig. 1b). The human heel pad also cushions impact transients, but to a lesser extent[5,10,11], raising the question of how runners struck the ground before the invention of modern running shoes. Previous studies have found that habitually shod runners tend to adopt a flatter foot placement when barefoot than when shod, thus reducing stresses on the foot[12–15], but there have been no detailed studies of foot kinematics and impact transients in long-term habitually barefoot runners.

We compared foot strike kinematics on tracks at preferred endurance running speeds (4–6 m s^{-1}) among five groups controlled for age and habitual footwear usage (Methods and Supplementary Data 2). Adults were sampled from three groups of individuals who run a minimum of 20 km per week: (1) habitually shod athletes from the USA; (2) athletes from the Rift Valley Province of Kenya (famed for endurance running[16]), most of whom grew up barefoot but now wear cushioned shoes when running; and (3) US runners who grew up shod but now habitually run barefoot or in minimal footwear. We also compared adolescents from two schools in the Rift Valley Province: one group (4) who have never worn shoes; and another group (5) who have been habitually shod most of their lives. Speed, age and distance run per week were not correlated significantly with strike type or foot and ankle angles within or among groups. However, because the preferred speed was approximately 1 m s^{-1} slower in indoor trials than in outdoor trials, we made statistical comparisons of kinematic and kinetic data only between groups 1 and 3 (Table 1).

Strike patterns vary within subjects and groups, but these trials (Table 1 and Supplementary Data 6) confirm reports[2,3,9] that habitually shod runners who grew up wearing shoes (groups 1 and 5) mostly RFS when shod; these runners also predominantly RFS when barefoot on the same hard surfaces, but adopt flatter foot placements by dorsiflexing approximately 7–10° less (analysis of variance, $P < 0.05$). In contrast, runners who grew up barefoot or switched to barefoot running (groups 2 and 4) most often used FFS landings followed by heel contact (toe–heel–toe running) in both barefoot and shod conditions. MFS landings were sometimes used in barefoot conditions (group 4)

[1]Department of Human Evolutionary Biology, 11 Divinity Avenue, [2]School of Engineering and Applied Sciences, Harvard University, Cambridge, Massachusetts 02138, USA. [3]University of Michigan Medical School, Ann Arbor, Michigan 48109, USA. [4]Center for Restorative and Regenerative Medicine, Providence Veterans Affairs Medical Center, Providence, Rhode Island 02906, USA. [5]Department of Physical Therapy, University of Delaware, Newark, Delaware 19716, USA. [6]Department of Medical Physiology, Moi University Medical School, PO Box 4606, 30100 Eldoret, Kenya. [7]Faculty of Biomedical & Life Sciences, University of Glasgow, Glasgow G12 8QQ, UK.
*These authors contributed equally to this work.

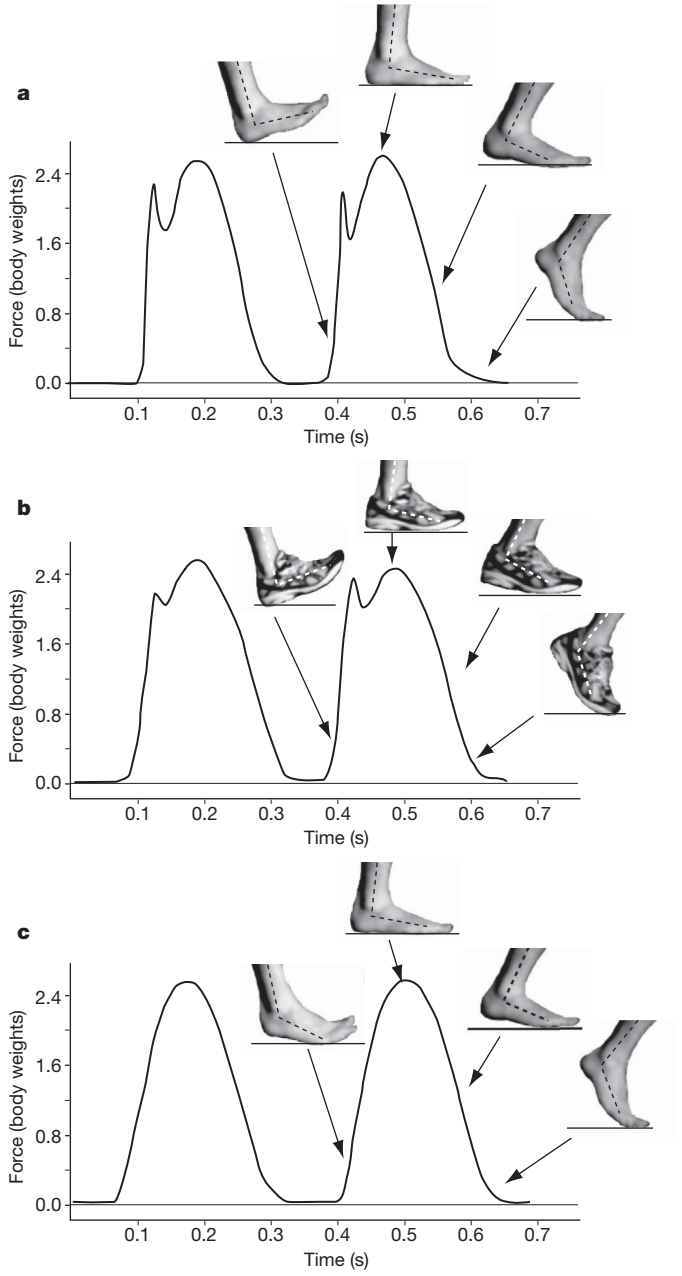

Figure 1 | Vertical ground reaction forces and foot kinematics for three foot strikes at 3.5 m s^{-1} in the same runner. **a**, RFS during barefoot heel–toe running; **b**, RFS during shod heel–toe running; **c**, FFS during barefoot toe–heel–toe running. Both RFS gaits generate an impact transient, but shoes slow the transient's rate of loading and lower its magnitude. FFS generates no impact transient even in the barefoot condition.

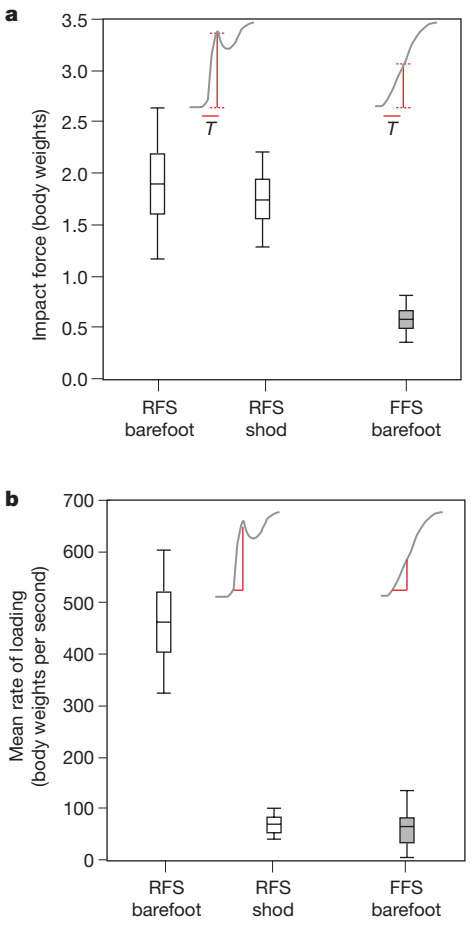

Figure 2 | Variation in impact transients. **a**, **b**, Magnitude (**a**) and rate of loading (**b**) of impact transient in units of body weight for habitually shod runners who RFS (group 1; open boxes) and habitually barefoot runners who FFS when barefoot (group 3; shaded boxes). The rate of loading is calculated from 200 N to 90% of the impact transient (when present) or to 6.2 ± 3.7% (s.d.) of stance phase (when impact transient absent). The impact force is 0.58 ± 0.21 bodyweights (s.d.) in barefoot runners who FFS, which is three times lower than in RFS runners either barefoot (1.89 ± 0.72 body weights (s.d.)) or in shoes (1.74 ± 0.45 body weights (s.d.)). The average rate of impact loading for barefoot runners who FFS is 64.6 ± 70.1 body weights per second (s.d.), which is similar to that for shod RFS runners (69.7 ± 28.7 body weights per second (s.d.)) and seven times lower than that for shod runners who RFS when barefoot (463.1 ± 141.0 body weights per second (s.d.)). The nature of the measurement (force versus time) is shown schematically by the grey and red lines. Boxes, mean ± s.d.; whiskers, mean ± 2 s.d.

and shod conditions (group 2), but RFS landings were infrequent during barefoot running in both groups. A major factor contributing to the predominance of RFS landings in shod runners is the cushioned sole of most modern running shoes, which is thickest below the heel, orienting the sole of the foot so as to have about 5° less dorsiflexion than does the sole of the shoe, and allowing a runner to RFS comfortably (Fig. 1). Thus, RFS runners who dorsiflex the ankle at impact have shoe soles that are more dorsiflexed relative to the ground, and FFS runners who plantarflex the ankle at impact have shoe soles that are flatter (less plantarflexed) relative to the ground, even when knee and ankle angles are not different (Table 1). These data indicate that habitually unshod runners RFS less frequently, and that shoes with elevated, cushioned heels facilitate RFS running (Supplementary Data 3).

Kinematic differences among foot strikes generate markedly different collision forces at the ground, which we compared in habitually shod and barefoot adult runners from the USA during RFS and FFS running (Methods and Supplementary Data 2). Whereas RFS landings cause large impact transients in shod runners and even larger transients in unshod runners (Fig. 1a, b), FFS impacts during toe–heel–toe gaits typically generate ground reaction forces lacking a distinct transient (Fig. 1c), even on a stiff steel force plate[4,17–19]. At similar speeds, magnitudes of peak vertical force during the impact period (6.2 ± 3.7% (all uncertainties are s.d. unless otherwise indicated) of stance for RFS runners) are approximately three times lower in habitual barefoot runners who FFS than in habitually shod runners who RFS either barefoot or in shoes (Fig. 2a). Also, over the same percentage of stance the average rate of loading in FFS runners when barefoot is seven times lower than in habitually shod runners who RFS when barefoot, and is similar to the rate of loading of shod RFS runners (Fig. 2b). Further, in the majority of barefoot FFS runners, rates of loading were approximately half those of shod RFS runners.

Modelling the foot and leg as an L-shaped double pendulum that collides with the ground (Fig. 3a) identifies two biomechanical factors,

namely the initial point of contact and ankle stiffness, that decrease M_{eff} and, hence, the magnitude of the impact transient (equation (1) and Supplementary Data 4). A RFS impact typically occurs just below the ankle, under the centre of mass of the foot plus leg, and with variable plantarflexion (Fig. 3b). Therefore, the ankle converts little translational energy into rotational energy and most of the translational kinetic energy is lost in the collision, leading to an increase in M_{eff} (ref. 20). In contrast, a FFS impact occurs towards the front of the foot (Fig. 3a), and the ankle dorsiflexes as the heel drops under control of the triceps surae muscles and the Achilles tendon (Fig. 3b). The ground reaction force in a FFS therefore torques the foot around the ankle, which reduces M_{eff} by converting part of the lower limb's translational kinetic energy into rotational kinetic energy, especially in FFS landings with low ankle stiffness (Fig. 3a). We note that MFS landings with intermediate contact points are predicted to generate intermediate M_{eff} values.

The conservation of angular impulse momentum during a rigid plastic collision can be used to predict M_{eff} as a function of the location of the centre of pressure at impact for ankles with zero and infinite joint stiffnesses (Supplementary Data 4). Figure 3 shows model values of M_{eff} for an average foot and shank comprising 1.4% and 4.5% M_{body}, respectively, where the shank is 1.53 times longer than the foot[21]. M_{eff} can be calculated, using experimental data from equation (1), as

$$M_{eff} = \frac{\int_{0^-}^{T} F_z(t)\,dt}{-v_{foot} + gT} \quad (2)$$

Using equation (2) with kinematic and kinetic data from groups 1 and 3 (Methods), we find that M_{eff} averages 4.49 ± 2.24 kg for RFS runners in the barefoot condition and 1.37 ± 0.42 kg for habitual barefoot runners who FFS (Fig. 3a). Normalized to M_{body}, the average M_{eff} is 6.8 ± 3.0% for barefoot RFS runners and 1.7 ± 0.4% for barefoot FFS runners. For all RFS landings, these values are not significantly different from the predicted M_{eff} values for a rigid ankle (5.5–5.9% M_{body}) or a compliant ankle (3.4–5.9% M_{body}), indicating that ankle compliance has little effect and that there is some contribution from mass above the knee, which is very extended in these runners (Fig. 3b). For FFS landings, M_{eff} values are smaller than the predicted values for a rigid ankle (2.7–4.1% M_{body}) and are insignificantly greater than those predicted for a compliant ankle (0.45–1.1% M_{body}), suggesting low levels of ankle stiffness. These results therefore support the prediction that FFS running generates collisions with a much lower M_{eff} than does RFS running. Furthermore, MFS running is predicted to generate intermediate M_{eff} values with a strong dependence on the centre of pressure at impact and on ankle stiffness.

How runners strike the ground also affects vertical leg compliance, defined as the drop in the body's centre of mass relative to the vertical force during the period of impact. Vertical compliance is greater in FFS running than in RFS running, leading to a lower rate of loading (Fig. 3c). More compliance during the impact period in FFS runners is partly explained by a 74% greater drop in the centre of mass (*t*-test, $P < 0.009$), resulting, in part, from ankle dorsiflexion and knee flexion (Fig. 3b). In addition, like shod runners, barefoot runners adjust leg stiffness depending on surface hardness[22]. As a result, we found no significant differences in rates or magnitudes of impact loading in barefoot runners on hard surfaces relative to cushioned surfaces (Supplementary Data 5).

Differences between RFS and FFS running make sense from an evolutionary perspective. If endurance running was an important behaviour before the invention of modern shoes, then natural selection is expected to have operated to lower the risk of injury and discomfort when barefoot or in minimal footwear. Most shod runners today land on their heels almost exclusively. In contrast, runners who cannot or prefer not to use cushioned shoes with elevated heels often avoid RFS landings and thus experience lower impact transients than do most shod runners today, even on very stiff surfaces (Fig. 2). Early

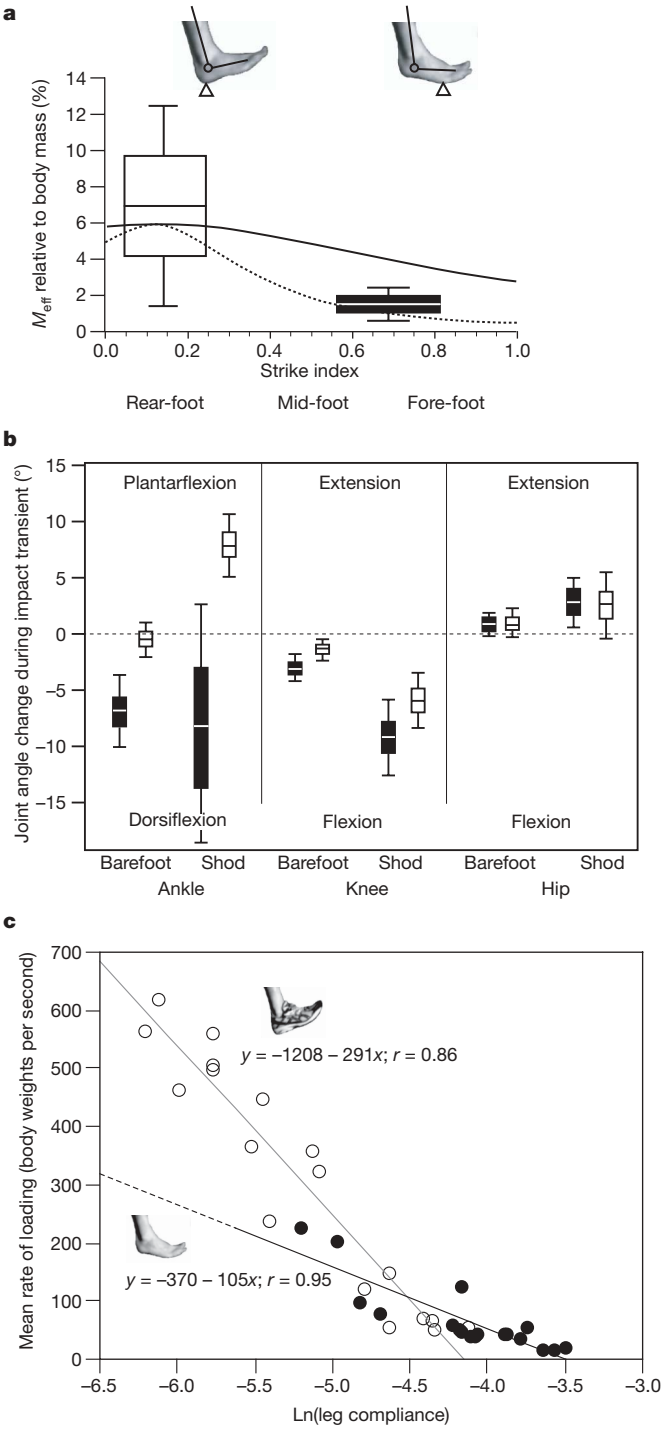

Figure 3 | Differences during impact between shod RFS runners (group 1) and barefoot FFS runners (group 3) at approximately 4 m s^{-1}. **a**, Predicted (lines) and measured (boxes) effective mass, M_{eff}, relative to body mass, versus foot length at impact (strike index) for FFS and RFS runners in the barefoot condition (Methods). The solid and dotted lines show predicted M_{eff} values for infinitely stiff and infinitely compliant ankles, respectively, at different centres of pressure. **b**, During the impact period, FFS runners (filled boxes) dorsiflex the ankle rather than plantarflexing it, and have more ankle and knee flexion than do RFS runners (open boxes). Boxes, mean ± s.d.; whiskers, mean ± 2 s.d. **c**, Overall dimensionless leg compliance (natural logarithm) during the impact-transient period (ratio of vertical hip drop relative to leg length at 90% of impact transient peak, normalized by body weight) relative to the rate of impact loading (body weights per second) for RFS runners (open circles) and FFS runners (filled circles) (shod and unshod conditions). Compliance is greater and is correlated with lower rates of loading in FFS impacts than in RFS impacts (plotted lines determined by least-squares regression; *r*, Pearson's correlation coefficient).

Table 1 | Foot strike type and joint angles of habitual barefoot and shod runners from Kenya and the USA

Group	*N* (male/female)	Age (age shod) (yr)	Strike-type mode (%)*				Joint angle at foot strike			Speed ($m\,s^{-1}$)
			Condition	RFS	MFS	FFS	Plantar foot†	Ankle†	Knee	
(1) Habitually shod adults, USA‡	8 (6/2)	19.1 ± 0.4 (<2)	Barefoot	83	17	0	−16.4 ± 4.4°	0.2 ± 3.0°	12.1 ± 7.9°	4.0 ± 0.3
			Shod	100	0	0	−28.3 ± 6.2°	−9.3 ± 6.5°	9.1 ± 6.4°	4.2 ± 0.3
(2) Recently shod adults, Kenya	14 (13/1)	23.1 ± 3.5 (12.4 ± 5.6)	Barefoot	9	0	91	3.7 ± 9.8°	18.6 ± 7.7°	21.2 ± 4.4°	5.9 ± 0.6
			Shod	29	18	54	−1.8 ± 7.4°	15.0 ± 6.7°	22.2 ± 4.3°	5.7 ± 0.6
(3) Habitually barefoot adults, USA§	8 (7/1)	38.3 ± 8.9 (<2)	Barefoot	25	0	75	8.4 ± 4.4°	17.6 ± 5.8°	17.3 ± 2.5°	3.9 ± 0.4
			Shod	50	13	37	−2.2 ± 14.0°	8.1 ± 15.9°	16.6 ± 2.4°	4.0 ± 0.3
(4) Barefoot adolescents, Kenya	16 (8/8)	13.5 ± 1.4 (never)	Barefoot	12	22	66	1.13 ± 6.8°	14.6 ± 8.3°	22.8 ± 5.4°	5.5 ± 0.5
			Shod‖	—	—	—	—	—	—	—
(5) Shod adolescents, Kenya	17 (10/7)	15.0 ± 0.8 (<5)	Barefoot	62	19	19	−10.1 ± 9.7°	4.1 ± 10.9°	18.9 ± 6.5°	5.1 ± 0.5
			Shod	97	3	0	−19.8 ± 10.3°	−2.7 ± 9.0°	18.4 ± 6.6°	4.9 ± 0.5

Data shown as mean ± s.d.
* RFS equivalent to heel-toe running; FFS equivalent to toe–heel–toe running.
† Angle of the sole of the foot or shoe (column 8), or of the ankle (column 9), relative to ground. Negative values indicate dorsiflexion relative to standing position; positive values indicate plantarflexion relative to standing position.
‡ Joint angles calculated from RFS only.
§ Joint angles calculated from FFS only.
‖ No shod condition reported because subjects had never worn shoes.

bipedal hominins such as *Australopithecus afarensis* had enlarged calcaneal tubers and probably walked with a RFS[23]. However, they lacked some derived features of the modern human foot, such as a strong longitudinal arch[1,24] that functionally improves the mass–spring mechanics of running by storing and releasing elastic energy[25]. We do not know whether early hominins ran with a RFS, a MFS or a FFS gait. However, the evolution of a strong longitudinal arch in genus *Homo* would increase performance more for non-RFS landings because the arch stretches passively during the entire first half of stance in FFS and MFS gaits. In contrast, the arch can stretch passively only later in stance during RFS running, when both the fore-foot and the rear-foot are on the ground. This difference may account for the lower cost of barefoot running relative to shod running[15,26].

Evidence that barefoot and minimally shod runners avoid RFS strikes with high-impact collisions may have public health implications. The average runner strikes the ground 600 times per kilometre, making runners prone to repetitive stress injuries[6–8]. The incidence of such injuries has remained considerable for 30 years despite technological advancements that provide more cushioning and motion control in shoes designed for heel–toe running[27–29]. Although cushioned, high-heeled running shoes are comfortable, they limit proprioception and make it easier for runners to land on their heels. Furthermore, many running shoes have arch supports and stiffened soles that may lead to weaker foot muscles, reducing arch strength. This weakness contributes to excessive pronation and places greater demands on the plantar fascia, which may cause plantar fasciitis. Although there are anecdotal reports of reduced injuries in barefoot populations[30], controlled prospective studies are needed to test the hypothesis that individuals who do not predominantly RFS either barefoot or in minimal footwear, as the foot apparently evolved to do, have reduced injury rates.

METHODS SUMMARY

We studied five subject groups (Table 1 and Supplementary Data 1), both barefoot and in running shoes. Habitually shod and barefoot US subjects ran over a force plate embedded 80% of the way along a 20–25-m-long indoor track. We quantified joint angles using a three-dimensional infrared kinematic system (Qualysis) at 240 Hz and a 500-Hz video camera (Fastec InLine 500M). African subjects were recorded on a 20–25-m outdoor track of hard dirt using a 500-Hz video camera. All subjects ran at preferred speeds with several habituation trials before each condition, and were recorded for five to seven trials per condition. We taped kinematic markers on joints and segments in all subjects. Video frames were analysed using IMAGEJ (http://rsb.info.nih.gov/nih-image/) to measure the angle of the plantar surface of the foot relative to earth horizontal (plantar foot angle), as well as ankle, knee and hip angles (Methods). We recorded the vertical ground reaction force (F_z) in US subjects at 4,800 Hz using AMTI force plates (BP400600 Biomechanics Force Platform), and normalized the results to body weight. The impact-transient magnitude and percentage of stance were measured at peak, and the rate of loading was quantified between 200 N and 90% of peak (following ref. 18). When there was no distinct impact transient, the same parameters were measured at the same percentage of stance plus/minus 1 s.d. as determined for each condition in trials with an impact transient. The effective mass (M_{eff}) in RFS runners was calculated using the integral of F_z (equation (2)) between the time when F_z exceeded 4 s.d. above baseline noise and the time when the transient peak was reached as measured in RFS runners; the impulse over the same percentage of stance (6.2 ± 3.7%) was used to calculated M_{eff} in FFS runners. Vertical foot and leg speed were calculated using a central difference method and the three-dimensional kinematic data.

Full Methods and any associated references are available in the online version of the paper at www.nature.com/nature.

Received 27 July; accepted 26 November 2009.
Published online XX 2010.

1. Bramble, D. M. & Lieberman, D. E. Endurance running and the evolution of *Homo*. *Nature* **432,** 345–352 (2004).
2. Kerr, B. A., Beauchamp, L., Fisher, V. & Neil, R. in *Proc. Int. Symp. Biomech. Aspects Sports Shoes Playing Surf.* (eds Nigg, B. M. & Kerr, B. A.) 135–142 (Calgary Univ. Press, 1983).
3. Hasegawa, H., Yamauchi, T. & Kraemer, W. J. Foot strike patterns of runners at 15-km point during an elite-level half marathon. *J. Strength Cond. Res.* **21,** 888–893 (2007).
4. Bobbert, M. F., Schamhardt, H. C. & Nigg, B. M. Calculation of vertical ground reaction force estimates during running from positional data. *J. Biomech.* **24,** 1095–1105 (1991).
5. Chi, K. J. & Schmitt, D. Mechanical energy and effective foot mass during impact loading of walking and running. *J. Biomech.* **38,** 1387–1395 (2005).
6. Milner, C. E., Ferber, R., Pollard, C. D., Hamill, J. & Davis, I. S. Biomechanical factors associated with tibial stress fractures in female runners. *Med. Sci. Sports Exerc.* **38,** 323–328 (2006).
7. Pohl, M. B., Hamill, J. & Davis, I. S. Biomechanical and anatomical factors associated with a history of plantar fasciitis in female runners. *Clin. J. Sport Med.* **19,** 372–376 (2009).
8. van Gent, R. N. *et al.* Incidence and determinants of lower extremity running injuries in long distance runners: a systematic review. *Br. J. Sports Med.* **41,** 469–480 (2007).
9. Nigg, B. R. *The Biomechanics of Running Shoes* (Human Kinetics, 1986).
10. Ker, R. F., Bennett, M. B., Alexander, R. M. & Kester, R. C. Foot strike and the properties of the human heel pad. *Proc. Inst. Mech. Eng. H* **203,** 191–196 (1989).
11. De Clercq, D., Aerts, P. & Kunnen, M. The mechanical characteristics of the human heel pad during foot strike in running: an *in vivo* cineradiographic study. *J. Biomech.* **27,** 1213–1222 (1994).
12. De Wit, B., De Clercq, D. & Aerts, P. Biomechanical analysis of the stance phase during barefoot and shod running. *J. Biomech.* **33,** 269–278 (2000).
13. Divert, C., Mornieux, G., Baur, H., Mayer, F. & Belli, A. Mechanical comparison of barefoot and shod running. *Int. J. Sports Med.* **26,** 593–598 (2005).
14. Eslami, M., Begon, M., Farahpour, N. & Allard, P. Forefoot-rearfoot coupling patterns and tibial internal rotation during stance phase of barefoot versus shod running. *Clin. Biomech. (Bristol, Avon)* **22,** 74–80 (2007).
15. Squadrone, R. & Gallozi, C. Biomechanical and physiological comparison of barefoot and two shod conditions in experienced barefoot runners. *J. Sports Med. Phys. Fitness* **49,** 6–13 (2009).
16. Onywera, V. O., Scott, R. A., Boit, M. K., &. Pitsiladis, Y. P. Demographic characteristics of elite Kenyan runners. *J. Sports Sci.* **24,** 415–422 (2006).
17. Dickinson, J. A., Cook, S. D. & Leinhardt, T. M. The measurement of shock waves following heel strike while running. *J. Biomech.* **18,** 415–422 (1985).
18. Williams, D. S., McClay, I. S. & Manal, K. T. Lower extremity mechanics in runners with a converted forefoot strike pattern. *J. Appl. Biomech.* **16,** 210–218 (2000).

19. Laughton, C. A., Davis, I. & Hamill, J. Effect of strike pattern and orthotic intervention on tibial shock during running. *J. Appl. Biomech.* **19,** 153–168 (2003).
20. Chatterjee, A. & Garcia, M. Small slope implies low speed for McGeers' passive walking machines. *Dyn. Syst.* **15,** 139–157 (2000).
21. Dempster, W. T. *Space Requirements of the Seated Operator: Geometrical, Kinematic, and Mechanical Aspects of the Body, with Special Reference to the Limbs*. WADC Technical Report 55-159 (United States Air Force, 1955).
22. Dixon, S. J., Collop, A. C. & Batt, M. E. Surface effects on ground reaction forces and lower extremity kinematics in running. *Med. Sci. Sports Exerc.* **32,** 1919–1926 (2000).
23. Latimer, B. & Lovejoy, C. O. The calcaneus of *Australopithecus afarensis* and its implications for the evolution of bipedality. *Am. J. Phys. Anthropol.* **78,** 369–386 (1989).
24. Jungers, W. L. *et al.* The foot of *Homo floresiensis. Nature* **459,** 81–84 (2009).
25. Ker, R. F., Bennett, M. B., Bibby, S. R., Kester, R. C. & Alexander, R. M. The spring in the arch of the human foot. *Nature* **325,** 147–149 (1987).
26. Divert, C. *et al.* Barefoot-shod running differences: shoe or mass effect. *Int. J. Sports Med.* **29,** 512–518 (2008).
27. Marti, B. in *The Shoe in Sport* (ed. Segesser, B.) 256–265 (Yearbook Medical, 1989).
28. Richards, C. E., Magin, P. J. & Calister, R. Is your prescription of distance running shoes evidence-based? *Br. J. Sports Med.* **43,** 159–162 (2009).
29. van Mechelen, W. Running injuries: a review of the epidemiological literature. *Sports Med.* **14,** 320–335 (1992).
30. Robbins, S. E. & Hanna, A. M. Running-related injury prevention through barefoot adaptations. *Med. Sci. Sports Exerc.* **19,** 148–156 (1987).

Supplementary Information is linked to the online version of the paper at www.nature.com/nature.

Acknowledgements We are grateful to the many volunteer runners who donated their time and patience. For help in Kenya, we thank M. Sang; E. Anjilla; Moi University Medical School; E. Maritim; and the students and teachers of Pemja, Union and AIC Chebisaas schools, in Kenya. For laboratory assistance in Cambridge, we thank A. Biewener, S. Chester, C. M. Eng, K. Duncan, C. Moreno, P. Mulvaney, N. T. Roach, C. P. Rolian, I. Ros, K. Whitcome and S. Wright. We are grateful to A. Biewener, D. Bramble, J. Hamill, H. Herr, L. Mahadevan and D. Raichlen for discussions and comments. Funding was provided by the US National Science Foundation, the American School of Prehistoric Research, The Goelet Fund, Harvard University and Vibram USA.

Author Contributions D.E.L. wrote the paper with substantial contributions from M.V., A.I.D., W.A.W., I.S.D., R.O.M. and Y.P. Collision modelling was done by M.V. and D.E.L.; US experimental data were collected by A.I.D., W.A.W. and D.E.L., with help from S.D'A. Kenyan data were collected by D.E.L., A.I.D., W.A.W., Y.P. and R.O.M. Analyses were done by A.I.D., D.E.L., M.V. and W.A.W.

Author Information Reprints and permissions information is available at www.nature.com/reprints. The authors declare competing financial interests: details accompany the full-text HTML version of the paper at www.nature.com/nature. Correspondence and requests for materials should be addressed to D.E.L. (danlieb@fas.harvard.edu).

METHODS

Subjects. We used five groups of subjects (outlined in Table 1 and Supplemental Table 1), including the following three groups of adults. Group 1 comprised amateur and collegiate athletes from the Harvard University community, recruited by word of mouth, all of whom were habitually shod since early childhood. Group 2 comprised Kalenjin athletes from the Rift Valley Province of Kenya, all training for competition, and recruited by word of mouth in the town of Kapsabet and at Chepkoilel Stadium, Eldoret. All adult Kenyan subjects were habitually shod, but 75% did not start wearing shoes and training in running shoes until late adolescence. Group 3 comprised self-identified habitual barefoot runners from the USA, recruited through the internet, who run either barefoot and/or in minimal footwear such as Vibram FiveFingers shoes, defined as lacking arch support and cushioning. In addition, two groups of adolescent subjects (aged 11–16 yr) were sampled from two schools in the Kalenjin-speaking region of Kenya. Group 4 comprised habitually unshod runners ($N = 16$; eight male, eight female) recruited from a rural primary school in the South Nandi District of Kenya in which none of children have ever worn shoes (verified by observation and interviews with teachers at the school). Group 5 comprised habitually shod runners ($N = 16$; nine male, seven female) recruited from an urban primary school in Eldoret in which all of the children have been habitually shod since early childhood.

For all adults, criteria for inclusion in the study included a minimum of 20 km per week of distance running and no history of significant injury during the previous six months. Habitual barefoot runners were included if they had run either barefoot or in minimal footwear for more than six months and if more than 66% of their running was either barefoot or in minimal footwear. To compare habitual barefoot FFS (toe–heel–toe) runners and habitually shod RFS (heel–toe) runners, we analysed kinematic and kinetic data from subsamples of six RFS runners from group 1 and six FFS runners from group 3 in greater depth (Supplementary Data Table 1).

All information on subject running history was self-reported (with the assistance of teachers for the Kenyan adolescents). All subjects participated on a voluntary basis and gave their informed consent according to the protocols approved by the Harvard Institutional Review Board and, for Kenyan subjects, the Moi University Medical School. Subjects were not informed about the hypotheses tested before recording began.

Treatments. All subjects were recorded on flat tracks approximately 20–25-m long. Subjects in groups 1–3 and 5 were recorded barefoot and in running shoes. A neutral running shoe (ASICS GEL-CUMULUS 10) was provided for groups 1 and 3, but groups 2 and 5 ran in their own shoes. Subjects in group 4 were recorded only in the barefoot condition because they had never worn shoes. For groups 1 and 3, two force plates (see below) were embedded at ground level 80% of the way along the track, with a combined force-plate length of 1.2 m. Force plates were covered with grip tape (3M Safety-Walk Medium Duty Resilient Tread 7741), and runners were asked to practice running before recording began so that they did not have to modify their stride to strike the plates. Kenyan runners in groups 2, 4 and 5 were recorded on flat, outdoor dirt tracks (with no force plates) that were 20–25-m long and cleaned to remove any pebbles or debris. In all groups, subjects were asked to run at a preferred speed and were given several habituation trials before each data collection phase, and were recorded in five to seven trials per condition, with at least one minute's rest between trials to avoid fatigue.

Kinematics. To record angles in lateral view of the ankle, knee, hip and plantar surface of the foot, a high-speed video camera (Fastec InLine 500M, Fastec Imaging) was placed approximately 0.5 m above ground level between 2.0 and 3.5 m lateral to the recording region and set to record at 500 Hz. Circular markers were taped on the posterior calcaneus (at the level of the Achilles tendon insertion), the head of metatarsal V, the lateral malleolus, the joint centre between the lateral femoral epicondyle and the lateral tibial plateau (posterior to Gerdy's tubercle), the midpoint of the thigh between the lateral femoral epicondyle and the greater trochantor of the femur (in groups 2, 4 and 5); the greater trochantor of the femur (only in groups 1 and 3); and the lateral-most point on the anterior superior iliac spine (only in groups 1 and 3). We could not place hip and pelvis markers on adolescent Kenyan subjects (groups 4 and 5). IMAGEJ (http://rsb.info.nih.gov/nih-image/) was used to measure three angles in all subjects: (1) the plantar foot angle, that is, the angle between the earth horizontal and the plantar surface of the foot (calculated using the angle between the lines formed by the posterior calcaneus and metatarsal V head markers and the earth horizontal at impact, and corrected by the same angle during quiet stance); (2) the ankle angle, defined by the metatarsal V head, lateral malleolus and knee markers; (3) the knee angle, defined by the line connecting the lateral malleolus and the knee and the line connecting the knee and the thigh midpoint (or greater trochantor). Hip angle was also measured in groups 1 and 2 as the angle between the lateral femoral condyle, the greater trochantor and the anterior superior iliac spine. All angles were corrected against angles measured during a standing, quiet stance. Average measurement precision, determined by repeated measurements (more than five) on the same subjects was $\pm 0.26^\circ$.

Under ideal conditions, plantar foot angles greater than 0° indicate a FFS, angles less than 0° indicate a RFS (heel strike) and angles of 0° indicate a MFS. However, because of inversion of the foot at impact, lighting conditions and other sources of error, determination of foot strike type was also evaluated by visual examination of the high-speed video by three of us. We also note that ankle angles greater than 0° indicate plantarflexion and that angles less than 0° indicate dorsiflexion.

Additional kinematic data for groups 1 and 3 were recorded with a six-camera system (ProReflex MCU240, Qualysis) at 240 Hz. The system was calibrated using a wand with average residuals of <1 mm for all cameras. Four infrared reflective markers were mounted on two 2-cm-long balsawood posts, affixed to the heel with two layers of tape following methods described in ref. 18. The average of these four markers was used to determine the total and vertical speeds of the foot before impact.

Kinetics. Ground reaction forces (GRFs) were recorded in groups 1 and 3 at 4,800 Hz using force plates (BP400600 Biomechanics Force Platform, AMTI). All GRFs were normalized to body weight. Traces were not filtered. When a distinct impact transient was present, transient magnitude and the percentage of stance was measured at peak; the rate of loading was quantified between 200 N and 90% of the peak (following ref. 18); the instantaneous rate of loading was quantified over time intervals of 1.04 ms. When no distinct impact transient was present, the same parameters were measured using the average percentage of stance ± 1 s.d. as determined for each condition in trials with an impact transient.

Estimation of effective mass. For groups 1 and 3, we used equation (2) to estimate the effective mass that generates the impulse at foot landing. The start of the impulse was identified as the instant at which the vertical GRF exceeded 4 s.d. of baseline noise above the baseline mean, and its end was chosen to be 90% of the impact transient peak (a 'real' time point among RFS runners, the average of which was used as the end of the transient in FFS runners who lacked a transient); this resulted in an impulse experienced, on average, through the first $6.2 \pm 3.7\%$ of stance. The integral of vertical GRF over the period of the impulse is the total impulse and was calculated using trapezoidal numerical integration within the MATLAB 7.7 environment using the TRAPZ function (Mathworks). Three-dimensional kinematic data of the foot (see above) were low-pass-filtered using a fourth-order Butterworth filter with a 25-Hz cut-off frequency. The vertical speed at the moment of impact was found by differentiating the smoothed vertical coordinate (smoothed with a piecewise-cubic Hermite interpolating polynomial) of the foot using numerical central difference. To minimize the effects of measurement noise, especially because we used differentiated data, we used the average of the three samples measured immediately before impact in calculating the impact speed. M_{eff} was then estimated as the ratio of the vertical GRF impulse (found by numerical integration) and the vertical impact speed (found by numerical differentiation).

SUPPLEMENTARY INFORMATION

1. Full Methods

Subjects

Five groups of subjects were used (outlined in Table 1 and Supplemental Table 1), including three groups of adults. Group 1: Habitually shod amateur and collegiate athletes from the Harvard University community, recruited by word of mouth, and all habitually shod since early childhood. Group 2: Adult athletes from the Rift Valley Province of Kenya, all training for competition, and recruited by word of mouth in the town of Kapsabet, Kenya; and at Chepkoilel Stadium, Eldoret Kenya. All adult Kenyan subjects were habitually shod, but 75% did not start wearing shoes and training in running shoes until late adolescence. Group 3: Self-identified habitual barefoot runners from the USA, recruited via the internet, who run either barefoot and/or in minimal footwear such as Vibram Five Finger® (VFF) shoes, defined as lacking arch support and cushioning. In addition, two groups of adolescent subjects (aged 11-16) were sampled from two schools in the Rift Valley Province, Kenya. Group 4: A habitually unshod group (N=16; 8 M, 8 F) was recruited from a rural primary school in the Nandi District in which none of children have ever worn shoes (verified by observation and interviews with teachers at the school). Group 5: A habitually shod group (N=16; 9 M, 7 F) was recruited from an urban primary school in Eldoret (Uasin Gishu District) in which all of the children have been habitually shod since early childhood.

For all adults, criteria for inclusion in the study included a minimum of 20 km per week of distance running, and no history of significant injury during the previous 6 months. Habitual barefoot runners were included if they had run either barefoot or in minimal footwear for more than six months, and if more than 66% of their running was either barefoot or in minimal footwear. In order to compare habitual barefoot forefoot strikers (toe-heel-toe runners) and habitually shod rearfoot strikers (heel-toe runners) , kinematic and kinetic data from subsamples of six rearfoot strikers from Group 1 and six forefoot strikers from Group 3 were analyzed in greater depth (see Supplementary Data Table 1).

All information on subject running history was self-reported (with the assistance of teachers for the Kenyan adolescents). All subjects participated on a voluntary basis

and gave their informed consent according to the protocols approved by the Harvard Institutional Review Board, and the Moi University Medical School (for Kenyan subjects). Subjects were not informed about the hypotheses tested prior to recording.

Treatments

All subjects were recorded on flat trackways, approximately 20-25 m long. Subjects in Groups 1-3, and 5 were recorded in barefoot and in running shoes. A neutral running shoe (Asics Gel-Cumulus 10) was provided for Groups 1 and 2, but Groups 3 and 5 ran in their own shoes; subjects in Group 4 were recorded only in the barefoot condition because they had never worn shoes. For Groups 1 and 3, two force plates (see below) were embedded at ground level 80% along the trackway, with a combined force plate length of 1.2 m. Force plates were covered with grip tape (3M Safety Walk, Medium Duty Tread 7741), and runners were asked to practice running prior to recording so that they did not have to modify their stride to strike the plates. Kenyan runners in groups 2, 4,5 were recorded on flat outdoor dirt trackways (with no force plate) that were 20-25 m long, cleaned to remove any pebbles or debris. In all groups, subjects were asked to run at a preferred speed and were given several habituation trials prior to each data collection phase, and they were recorded for 5-7 trials per condition with at least one minute rest between trials to avoid fatigue.

Kinematics

To record angles in lateral view of the ankle, knee, hip, and plantar surface of the foot, a high speed video camera (Fast-Tec Inline 500M, San Diego, CA) was placed approximately 0.5 m above ground level between 2.0 and 3.5 m lateral to the recording region (e.g., the force plate) and recorded at 500 Hz. Circular markers were taped on the posterior calcaneus (at the level of the Achilles tendon insertion), the head of metatarsal V, the lateral malleolus, the joint centre between the lateral femoral epicondyle and the lateral tibial plateau (posterior to Gerdy's tubercle), the midpoint of the thigh between the lateral femoral epicondyle and the greater trochantor of the femur (in Groups 2, 4,5); the greater trochantor of the femur (only in Groups 1 and 3); and the lateral-most point on the anterior superior iliac spine (only in Groups 1 and 3). We were not permitted to place hip and pelvis markers on adolescent Kenyan subjects (Groups 4 and 5). ImageJ

(http://rsb.info.nih.gov/nih-image/) was used to measure three angles in all subjects: (1) the plantar foot angle (PFA), the angle between the earth horizontal and the plantar surface of the foot (calculated using the angle between the lines formed by the posterior calcaneus and fifth metatarsal head markers and the earth horizontal at impact and corrected by the same angle during quiet stance); (2) ankle angle, defined by the fifth metatarsal head, lateral malleolus, and knee markers; (3) knee angle, defined by the line connecting the lateral malleolus and knee and the line connecting the knee and the thigh midpoint (or greater trochantor). Hip angle was also measured in Groups 1 and 2 as the angle between the lateral femoral condyle, the greater trochantor, and the anterior superior iliac spine. All angles were corrected against angles measured during a standing, quiet stance. Average measurement precision, determined by repeated measurements (>5) on the same subjects was ± 0.26°.

Under ideal conditions, PFA angles above 0° indicate a forefoot strike, angles below 0° indicate a rearfoot (heel) strike, and angles of 0° indicate a midfoot strike. However, because of inversion of the foot at impact, lighting conditions and other sources of error, determination of foot strike type was also evaluated by visual examination of the high speed video by three researchers. Note also that ankle angles greater than 0° indicate plantarflexion, and angles less than 0° indicate dorsiflexion.

Additional kinematic data for Groups 1 and 3 were recorded with a 6 camera Qualysis system (ProReflex MCU 240, Qualysis, Gothenburg, Sweden) at 240 Hz. The system was calibrated using a wand with average residuals < 1 mm for all cameras. Four infrared reflective markers were mounted on two 2 cm long balsawood posts, affixed to the heel with two layers of tape following methods described in Ref. 1. An average of these four markers was used to determine foot total and vertical velocity of the foot prior to impact.

Kinetics

Ground reaction forces (GRFs) were recorded in Groups 1 and 3 at 4,800 Hz using AMTI force plates (BP400600, Watertown, MA). All GRFs were normalized to body weight. Traces were not filtered. When a distinct impact transient was present, transient magnitude and the percentage of stance was measured at peak; the rate of loading (ROL) was quantified between 200 N and 90% of the peak (following Ref. 1);

instantaneous ROL was quantified over time intervals of 1.04 ms. When no distinct impact transient was present, the same parameters were measured using the average percentage of stance ±1 standard deviation as determined for each condition in trials with an impact transient.

Effective mass estimation

For Groups 1 and 3, we used equation 2 to estimate the effective mass that generates the impulse at foot landing. The start of the impulse was identified as the instant when the vertical GRF exceeded 4 s.d. of baseline noise above the baseline mean, and the end was chosen to be 90% of the impact transient peak (a "real" time point among rearfoot strike runners, the average of which was used as the end of the transient in FFS runners who lacked a transient); this results in an impulse experienced, on average, through the first 6.2% ± 3.7 s.d. of stance. The integral of vertical GRF over the time period of the impulse is the total impulse and was calculated using trapezoidal numerical integration within the Matlab 7.7 environment using the TRAPZ function (Mathworks Inc., Natick, MA). Three dimensional kinematic data of the foot (see *Kinematics*) were low pass filtered using a 4^{th} order Butterworth filter with a 25 Hz cutoff frequency. The vertical velocity at the moment of impact was found by differentiating the smoothed vertical coordinate (via a piecewise cubic Hermite interpolating polynomial) of the foot using numerical central difference. To minimize the effects of measurement noise, especially because we used differentiated data, we used the average of the three samples immediately prior to impact in calculating the impact velocity. M_{eff} was then estimated as the ratio of the vertical GRF impulse (found by numerical integration) to the vertical impact velocity (found by numerical differentiation).

1. Williams, D. S., McClay, I. S., & Manal, K. T. Lower extremity mechanics in runners with a converted forefoot strike pattern. J Appl. Biomech. **16**, 210-18 (2000).

Supplementary Data 2: Sample characteristics

Supplementary Table 1: Sample characteristics

Group	N (m/f)	Age ±s.d.	Age shod	Height (m) ±s.d.	Weight (kg) ±s.d.	Km run/day ±s.d.
Adults						
1. Habitual shod, USA	8 (6/2)	19.1 ±0.4	<2	1.71 ±0.10	64.4 ±6.7	12.0 ±6.5
2. Transitioned to shod, Kenya	14 (13/1)	23.1 ±3.5	12.4 ±5.6	1.72 ±0.09	55.1 ±6.4	22.0 ±7.4
3. Habitual barefoot, USA[1]	8 (7/1)	38.3 ±8.9	<2	1.80 ±0.07	77.2 ±13.3	8.3 ±4.1[1]
Adolescents						
4. Rural barefoot, Kenya	16 (8/8)	13.5 ±1.4	never	1.55 ±0.10	39.4 ±8.9	19.4[2] ±8.2
5. Urban shod, Kenya	16 (9/7)	15.0 ±0.8	<5	1.64 ±0.02	53.2 ±7.7	6.0[1] ±2.6[1]

[1]Among these runners, on average, 83% of training was in minimal shoes, 13% was barefoot, 4% was in cushioned, high-heeled running shoes.

[2]Estimated using average running speed, reported time spent running per day, and information provided by teachers.

Supplementary Data 3: Vibram FiveFinger™ Training Study

In order to test if and/or how habitually shod RFS runners change their strike when they transition from wearing running shoes to minimal footwear, we recruited 14 (10 male/4 female) subjects in 2008 and 2009 for a six week study. Subjects were solicited by email and word of mouth from the Harvard community. All subjects were habitual runners (>20 km run/week), with no lower limb or foot injuries. Average age was 21.4 years ± 1.8 s.d.; average weight was 68.3 kg ± 2.2 s.d.; average height was 170.1 cm ± 2.1 s.d.

Subjects were provided a pair of Vibram FiveFingers™ (FF, Sprint model) and asked to train for 6 weeks, keeping a log of their training. Subjects were asked to begin by running no more than 1.6 km/day in the FF shoes during the first week. They then increased the daily running distance by no more than 10-20% per week, to a maximum of 16-20 km/week. No subjects were paid, no subjects were instructed on how to run, and all gave their informed written consent as approved by the Harvard IRB.

Footstrike patterns were recorded prior to the study (Week 0) and at the end of the study (Week 6) using a high speed video camera (Fast-Tec Inline 500-M, San Diego, CA) at 500 Hz, and a Tekscan pressure pad (Tekscan HR Mat, South Boston, MA) at 250 Hz mounted along a 20 meter-long concrete floor trackway in the Peabody Museum (Harvard University, Cambridge, MA). Subjects were recorded for a minimum of 5 trials per condition to observe their modal footstrike pattern.

Kinematic results of these subjects (Supplementary Table 2, see Methods) showed that, on average, over the course of the 6 week training period the plantar angle of the foot at strike transitioned to being 7.2° ± 3.2 s.d. more plantarflexed ($p<0.05$), and average ankle angle at impact became more plantarflexed by 5.6° ± 3.6 s.d. ($p<0.05$).

Supplemental Data Table 2: Modal footstrike patterns among habitually shod runners who trained in Vibram FiveFinger® shoes

	Week 0	Week 6
Strike Type	(% subjects)	(% subjects)
Rearfoot strike	72	36
Midfoot strike	14	0
Forefoot strike[1]	14	57
Toe strike[2]	0	7

[1]defined as a forefoot strike followed by heel contact (toe-heel-toe running)

[2]defined as a forefoot strike with no heel contact

Supplementary Data 4: Modelling collisional impulse in different foot strike types

In this supplement we derive the equations for a rigid plastic collision of a L-shaped object (thus similar to the lower leg and foot) that either has an ankle-like hinge at the corner, or has no joint (i.e., a stiff ankle). With respect to the collision, 'rigid' refers to the assumption that the collision is instantaneous, and thus gives rise to infinitely large instantaneous forces over an infinitesimal time period so that the net impulse due to the force is finite. Because the duration of the collision is nearly zero, the configuration of the system remains constant over the period of the collision. The term plastic refers to the assumption that there is no rebound. This supplement is in two parts: the first part considers the collision of a L-shaped bar, i.e. a double pendulum with a fused joint; and the second part considers the collision of a L-shaped double pendulum with a frictionless hinge joint. These conditions therefore represent the two extremes of ankle joint stiffness, infinite and zero, respectively.

Notation

Plain roman variables (e.g., A) denote labels for points in a figure, italicized variables (e.g., A) denote scalars, underlined variables (e.g., $\underline{A}$) denote vectors, and bold roman variables (e.g., **A**) denote matrices. Vector notation such as $\underline{A}_{P/O}$ refers to a vector quantity at point P, measured with respect to point O; examples include position or velocity of P with respect to O. Unreferenced vectors such as $\underline{A}_P$ are simply measured with respect to the origin. Angular momentum and inertia are always measured with respect to a point, and therefore their notation is of the type $\underline{A}_{/O}$ to indicate that that the vector $\underline{A}$ is defined with respect to a point O. Superscripts – and + denote the instant of

time before and after contact, respectively (e.g., $\underline{v}^+$). The point G refers to the centre of mass of the entire object. Finally, unit vectors of the global inertial coordinate system are denoted using $\hat{i}$, $\hat{j}$ and $\hat{k}$ for the x, y and z axes, respectively, such that the object is confined to the x-y plane.

Condition I: Infinitely stiff ankle joint

For simplicity, we consider first the case of an L-shaped bar falling vertically downward with velocity $\underline{v}_G^- = -v^-\hat{j}$ and no rotational velocity, i.e. $\underline{\Omega}^- = 0$. Because of the collision, there is an abrupt jump in the angular and linear velocities of the L-shaped bar to give $\underline{v}_G^+$ and $\underline{\Omega}^+ = \omega^+\hat{k}$. Figure S4.1 shows a free body diagram of the L-shaped bar with the "foot" part in contact with the ground at a point O (centre of pressure) that is located between the tip of the foot and the ankle. The only external force-impulse on the L-bar is applied at O. Therefore for the angular impulse-momentum balance about O, there are no external torque-impulses acting on the L-shaped bar about O, and hence the angular momentum $\underline{H}_{/O}$ about O is the same before and after the collision. In terms of the angular velocity vector $\underline{\Omega}$, the velocity of the centre of mass G is given by:

$$\underline{v}_G = \underline{v}_O + \underline{\Omega} \times \underline{r}_{G/O} \tag{S4.1}$$

and note that $\underline{v}_O^- = -v^-\hat{j}$ and $\underline{v}_O^+ = 0$. Then, the angular impulse-momentum balance is expressed as $\underline{H}_{/O}^+ = \underline{H}_{/O}^-$ where:

$$\begin{aligned} \underline{H}_{/O}^- &= (m+M)\underline{r}_{G/O} \times \underline{v}_G^- \\ \underline{H}_{/O}^+ &= (m+M)\underline{r}_{G/O} \times \underline{v}_G^+ + \mathbf{I}_{/G}\underline{\Omega}^+ \end{aligned} \tag{S4.2}$$

and m is the mass of the foot, M is mass of the shank, and $\mathbf{I}_{/G}$ is the moment of inertia matrix of the foot plus shank about the centre of mass G, where only the principal inertia I_{zz} parallel to the z-axis is relevant for this planar object. Because the problem is

planar, the only non-zero component of the angular momentum vectors is the z-component, yielding one equation with one unknown, ω^+, which we can solve. We find $\underline{v}_G^+$ using equation S4.1 and linear impulse-momentum balance for the L-shaped bar gives us the impulse $\underline{J}$ at the contact point O as:

$$\underline{J} = (m + M)(\underline{v}_G^+ - \underline{v}_G^-) \tag{S4.3}$$

Therefore, the effective mass M_{eff} (equivalent to equation 2 from the main text) is given by:

$$M_{\text{eff}} = \left| \frac{\underline{J}.\hat{j}}{v^-} \right| \tag{S4.4}$$

By solving equations S2.2 to find ω^+, we find M_{eff} for a L-shaped bar (infinitely stiff ankle) that is falling vertically with a speed v^- as:

$$M_{\text{eff}} = \frac{l^2 m(m + 4M) + 4L^2 M(m + M)}{4(l^2(3s^2(m + M) - 3ms + m) + L^2 M)} \tag{S4.5}$$

where s is the strike index (distance from the heel to the centre of pressure at impact relative to total foot length), L and l are the shank's and foot's length, respectively. For generating the graph of M_{eff} as a function of the strike index, s, we use the mean values reported by Dempster (1955) to set m = 1.4% body mass, M = 4.5% body mass, and L = 1.53 l.

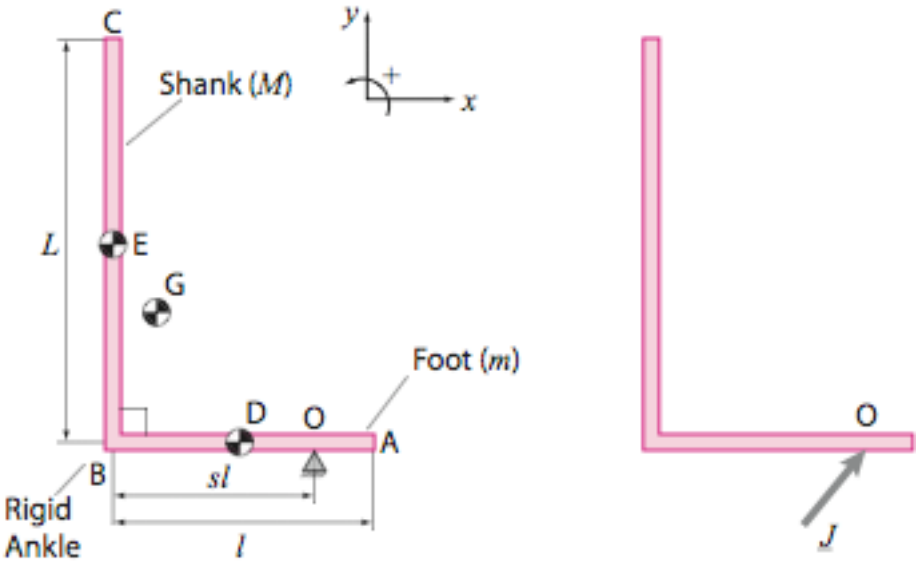

Supplementary Figure S4.1: A right angled L-shaped bar as a model of a foot plus shank having infinite ankle stiffness, and its free body diagram. In the collision free body diagram (right), only the impulse $\underline{J}$ due to the collision is shown because the impulse from gravitational forces vanishes in the limit of a rigid collision that happens instantaneously. We use angular impulse-momentum balance about the point O to find the jump in velocity of the L-shaped bar from the collision. Linear impulse-momentum balance is then used to find $\underline{J}$.

Condition II: Infinitely compliant ankle joint

Here we derive M_{eff} as a function of strike index, s, for conditions in which the corner of the L-shaped "bar" has a frictionless hinge, i.e. a double-pendulum with its joint flexed to 90° when it collides with the ground. This is analogous to an infinitely compliant ankle. Figure S4.2 shows the collision free body diagram for this posture of the double pendulum. We assume that, just before impact, the entire object is moving downward with speed v^- (i.e., $\underline{v}_{\text{D}}^- = \underline{v}_{\text{E}}^- = \underline{v}_{\text{G}}^- = -v^- \hat{j}$) and no angular velocity (i.e.,

$\underline{\Omega}_m^- = \underline{\Omega}_M^- = 0$). Assuming a rigid plastic collision, we use angular impulse-momentum balance of the entire double pendulum about the collision point O, and the shank segment (of mass M) about the hinge point B. The angular momentum vectors about O and B are given by:

$$\begin{aligned}
&\underline{H}_{m+M/\mathrm{O}} = \left(m\underline{r}_{\mathrm{D}/\mathrm{O}} \times \underline{v}_{\mathrm{D}} + \mathbf{I}_{m/\mathrm{D}}\underline{\Omega}_m\right) + \left(M\underline{r}_{\mathrm{E}/\mathrm{O}} \times \underline{v}_{\mathrm{E}} + \mathbf{I}_{M/\mathrm{E}}\underline{\Omega}_M\right) \\
&\underline{H}_{M/\mathrm{B}} = M\underline{r}_{\mathrm{E}/\mathrm{B}} \times \underline{v}_{\mathrm{E}} + \mathbf{I}_{M/\mathrm{E}}\underline{\Omega}_M \\
&\underline{v}_{\mathrm{D}} = \underline{v}_{\mathrm{O}} + \underline{\Omega}_m \times \underline{r}_{\mathrm{D}/\mathrm{O}} \\
&\underline{v}_{\mathrm{E}} = \underline{v}_{\mathrm{O}} + \underline{\Omega}_m \times \underline{r}_{\mathrm{B}/\mathrm{O}} + \underline{\Omega}_M \times \underline{r}_{\mathrm{E}/\mathrm{B}}
\end{aligned} \tag{S4.6}$$

where subscripts m, M and m+M refer to the two segments separately or together, and the only relevant element of the matrices **I** is the principal moment of inertia I_{zz} parallel to the z-axis. Because there are no external torques on the body about the points O and B, the angular impulse-momentum equations are:

$$\begin{aligned}
\underline{H}^+_{m+M/\mathrm{O}} &= \underline{H}^-_{m+M/\mathrm{O}} \\
\underline{H}^+_{M/\mathrm{B}} &= \underline{H}^-_{M/\mathrm{B}}
\end{aligned} \tag{S4.7}$$

Using the two non-zero z-components of the of the angular momentum vectors in equation S4.7 and with $\underline{v}_{\mathrm{O}}^- = -v^-\hat{j}$, $\underline{v}_{\mathrm{O}}^+ = 0$, we solve for the two unknown angular velocities of the segments $\underline{\Omega}_m^+ = \omega_m^+\hat{k}$ and $\underline{\Omega}_M^+ = \omega_M^+\hat{k}$ after the collision. Then, linear impulse-momentum balance of the entire system gives us the collisional impulse, $\underline{J}$, that is imparted at the point O as:

$$\begin{aligned}
\underline{J} &= (m+M)(\underline{v}_{\mathrm{G}}^+ - \underline{v}_{\mathrm{G}}^-) \\
\underline{v}_{\mathrm{G}} &= \underline{v}_{\mathrm{O}} + \frac{m\underline{v}_{\mathrm{D}} + M\underline{v}_{\mathrm{E}}}{m+M}
\end{aligned} \tag{S4.8}$$

Therefore, M_{eff} for the vertical impulse due to the collision is given by:

$$M_{\mathrm{eff}} = \left|\frac{\underline{J}.\hat{j}}{v^-}\right| = \frac{m(m+4M)}{4\left(3s^2(m+M) - 3ms + m\right)} \tag{S4.9}$$

Equations S4.5 and S4.9 are graphed in Figure 3a of the main text. The model presented here can be extended by considering rebound, friction, more segments to account for the thigh, torso, and so on. A detailed treatise on rigid body collisions can be found in Chatterjee, 1997. But to our knowledge, there has been no systematic analysis in the literature of how the ground reaction impulse is affected by the strike index, i.e. the point of collision of the distal segment.

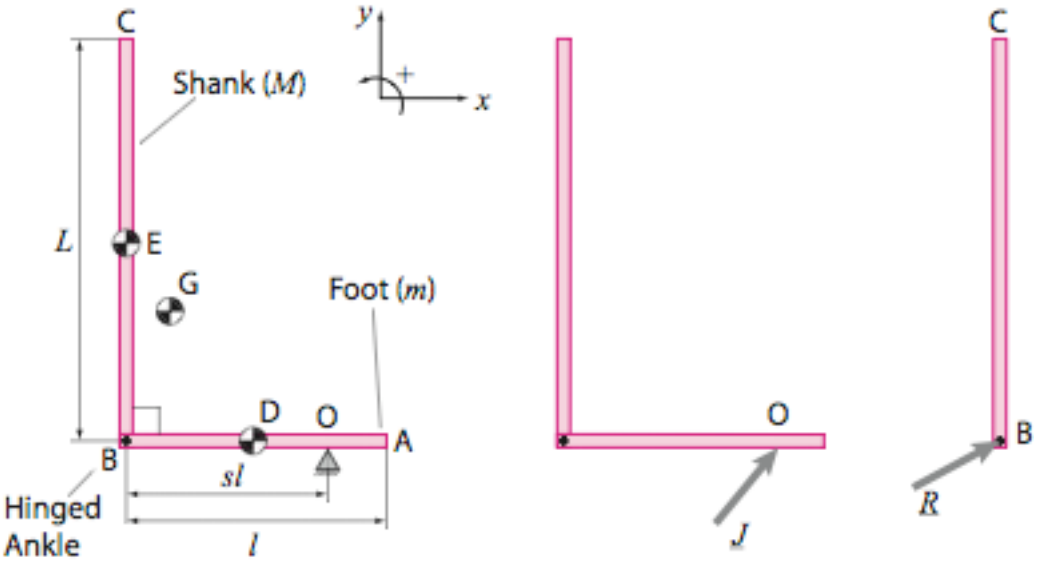

Supplementary Figure S4.2: A double pendulum with a frictionless hinge and 90° flexion as a model of a foot plus shank having infinite ankle compliance (zero stiffness), and the associated free body diagrams. We use angular impulse-momentum balance about O for the entire system, and balance about point B for the shank in order to find the jump in velocities arising from the collision. Gravitational impulses vanish in a rigid collision because it happens instantaneously. Finally, linear impulse-momentum balance for the whole system is used to calculate $\underline{J}$.

References

1. Chatterjee, A. Rigid body collisions: some general considerations, new collision laws, and some experimental data. Ph.D. Dissertation. *Cornell University*, 1997.

2. Dempster, W.T. Space Requirements of the seated operator. *WADC-Technical Report 55-159*, Wright-Patterson Air Force Base, Ohio (1955).

Supplementary Data 5. Comparison of impact transient data and leg compliance in padded versus unpadded conditions

In order to assess the effect of substrate stiffness, rearfoot strike and forefoot strike runners (Groups 1 and 3 from Table 1) were tested on the same trackway described above with and without a 1 cm thick layer of carpet padding (Plushstep Deluxe 0.375 cm, 6 lbs/cft density, 4.2 psi tensile strength, 45% elongation). Variables measured were impact transient magnitude (in body weights), average rate of loading (from 200N to 90% of the impact transient peak), and overall leg compliance (hip marker drop over the period of the impact transient normalized by 90% of the impact transient magnitude).

Results, illustrated in Supplementary Figure 2, show that runners adjust leg stiffness depending on surface hardness in both the shod and barefoot conditions as demonstrated in previous studies of shod subjects (Feehery, 1986; Dixon et al, 2000). Although habitually shod rearfoot strikers had significantly higher rates of loading without padding than with padding in the barefoot condition ($p<0.01$). However, their rates of loading when shod did not differ with or without padding. Additionally, their rates of loading were not significantly different from those of habitually barefoot forefoot strikers with or without padding (see main text). Habitual barefoot toe-heel-toe runners who forefoot strike actually had slightly lower (but not significantly different, $p=0.34$) magnitudes of loading during impact on hard versus cushioned surfaces; they also experienced significantly higher rates of loading when shod versus unshod ($p<0.05$).

These results therefore indicate that habitual barefoot runners who forefoot strike are not negatively affected by hard substrates, but instead have impact transient

characteristics that are similar or smaller than those experienced by shod runners under the same conditions.

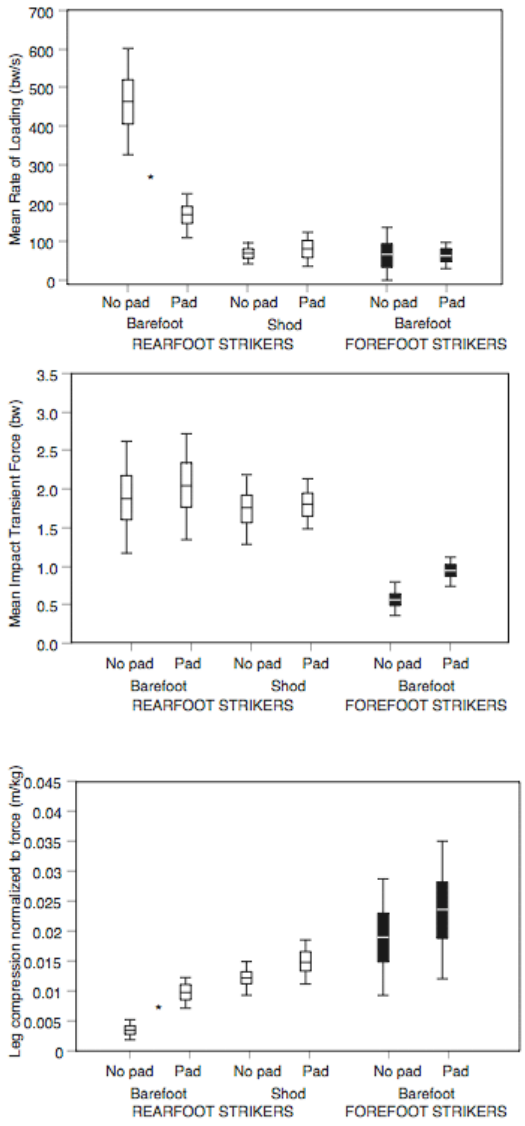

Supplementary Figure 2 Impact transient characteristics and overall leg compliance in padded versus unpadded conditions in habitual barefoot and shod runners (* indicates significant difference as determined by ANOVA).

Supplementary Data 6: Additional kinematic and anthropmetric information

1. Quicktime format movies of representative footstrikes:

-Movie 1: Adolescent Kalenjin female, habitually barefoot, unshod condition (forefoot strike)

-Movie 2: Adolescent Kalenjin male, habitually barefoot, unshod condition (forefoot strike)

-Movie 3: Adult Kalenjin runner, habitually barefoot until adolescence, unshod condition (forefoot strike)

-Movie 4: Adult Kalenjin runner, habitually barefoot until adolescence, shod condition (midfoot strike)

-Movie 5: Adolescent Kalenjin student, habitually shod, shod condition (rearfoot strike)

-Movie 6. Adolescent Kalenjin student, habitually shod, unshod condition (rearfoot strike)

-Movie 7: Pressure pad movie of forefoot strike (toe-heel-toe running)

-Movie 8: Pressure pad movie rearfoot strike (heel-toe running)

-Movie 9: Pressure pad movie of midfoot strike

2. Additional notes.

Running form prior to mid-1970s.

Empirical data on the prevalence of different footstrike patterns from long distance runners prior to the mid-1970s is difficult to obtain because most films and videos were made at insufficient speeds to capture the instant of foot strike precisely. Interviews with older runners and training manuals, however, all indicate that FFS running was the

predominant running style among middle and long distance runners. A typical summary of what was considered normal running style running from this era is exemplified by Fred Wilt's *How They Train 2nd Ed* (1973, Track and Field News, Los Altos, CA, pg 122): "The supporting phase beings with the forward foot beneath the body's center of gravity. The knee is bent as the outer border of the ball of the foot makes contact with the ground. Immediately thereafter the heel comes to the ground naturally, with no effort being made to prevent it from grounding. This applies to sprinting as well as middle and long-distance running."

Heel pad thickness. Examination by palpation of the foot indicates that habitually unshod subjects from Kenya (Group 4) had more calloused feet than age-matched habitually shod subjects (Group 5). Future study is necessary to measure the difference in callous and heel pad thickness. Additionally, habitual barefoot subjects informed us that they found the hard, dirt trackway (a dry dirt road) on which we recorded them a "very comfortable" and "easy" surface on which to run.

Incline. Footstrike patterns are variable depending not only on substrate hardness and texture, but also incline. Habitually shod runners typically FFS when running up an incline, and RFS when running on flat surfaces or down an incline. We have observed that habitual barefoot runners both in America and Kenya predominantly FFS when running downhill by increasing joint flexion of the knee and hip.